Supporting information

Upregulation of Robo4 expression by SMAD signaling suppresses vascular permeability and mortality in endotoxemia and COVID-19 models

Maaya Morita[1], Aki Yoneda[1], Nagisa Tokunoh[2,3], Tatsumi Masaki[1], Keisuke Shirakura[1], Mayumi Kinoshita[1], Rina Hashimoto[4], Naoya Shigesada[1], Junya Takahashi[1], Masashi Tachibana[1], Shota Tanaka[1], Masanori Obana[1,5], Nobumasa Hino[1], Masahito Ikawa[1,2,5], Kazutake Tsujikawa[1], Chikako Ono[2,5], Yoshiharu Matsuura[2,5], Hiroyasu Kidoya[6], Nobuyuki Takakura[2,5], Yoshiaki Kubota[7], Takefumi Doi[1], Kazuo Takayama[4], Yasuo Yoshioka[1,2,3,5], Yasushi Fujio[1,5], Yoshiaki Okada[1,5*]

[1]Graduate School of Pharmaceutical Sciences, Osaka University, Osaka 565-0871, Japan
[2]Research Institute for Microbial Diseases, Osaka University, Osaka 565-0871, Japan
[3]BIKEN Center for Innovative Vaccine Research and Development, The Research Foundation for Microbial Diseases of Osaka University, Osaka 565-0871, Japan
[4]Center for iPS Cell Research and Application (CiRA), Kyoto University, Kyoto 606-8507, Japan
[5]Center for Infectious Disease Education and Research (CiDER), Osaka University, Osaka 565-0871, Japan
[6]Department of Integrative Vascular Biology, Faculty of Medical Sciences, University of Fukui, 23-3 Matsuoka-Shimoaizuki, Eiheiji, Yoshida, Fukui 910-1193, Japan.
[7]Department of Anatomy, Keio University School of Medicine, Tokyo 160-8582, Japan.

*Correspondence to: **Yoshiaki Okada**, Ph.D., Graduate School of Pharmaceutical Sciences, Osaka University, 1-6 Yamadaoka, Suita, Osaka 565-0871, Japan
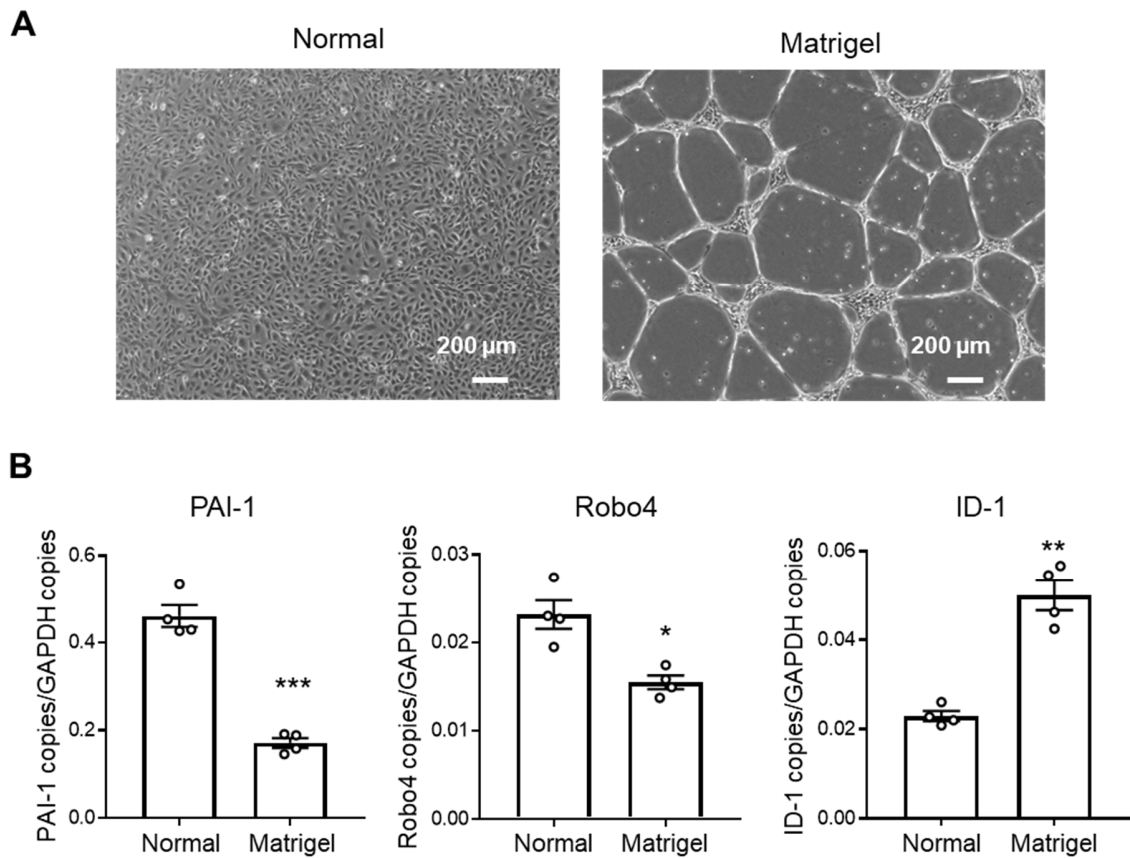Email: okadabos@phs.osaka-u.ac.jp

Figure S1. Culture condition-dependent expression levels of PAI-1, ID-1, and Robo4 in endothelial cells

(A) HUVECs cultured in the presence or absence of Matrigel. Pictures are representative images of HUVECs cultured in normal or Matrigel conditions. Scale bar = 200 μm. (B) Effect of Matrigel culture on PAI-1, Robo4, and ID-1 expression. HUVECs were cultured in the presence or absence of Matrigel for 24 h, and PAI-1, ID-1, and Robo4 expression was measured by qPCR (n = 4, $*p < 0.05$, $**p < 0.01$, by the unpaired t-test). Data are expressed as the mean ± standard error of the mean.
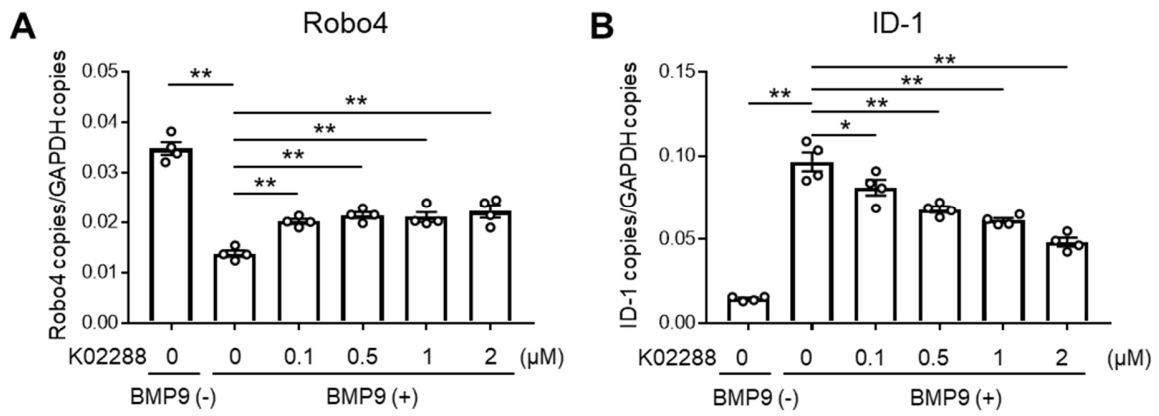
Figure S2. Expression levels of Robo4 and ID-1 in endothelial cells treated with K02288 and BMP9. HUVECs were treated with K02288 (0.1 to 2 µM) for 30 min followed by BMP9 (1 ng/mL). Expression levels of Robo4 (A) and ID-1 (B) were measured by qPCR (n = 4, *p < 0.05, **p < 0.01 by Tukey's test). Data are expressed as the mean ± standard error of the mean.
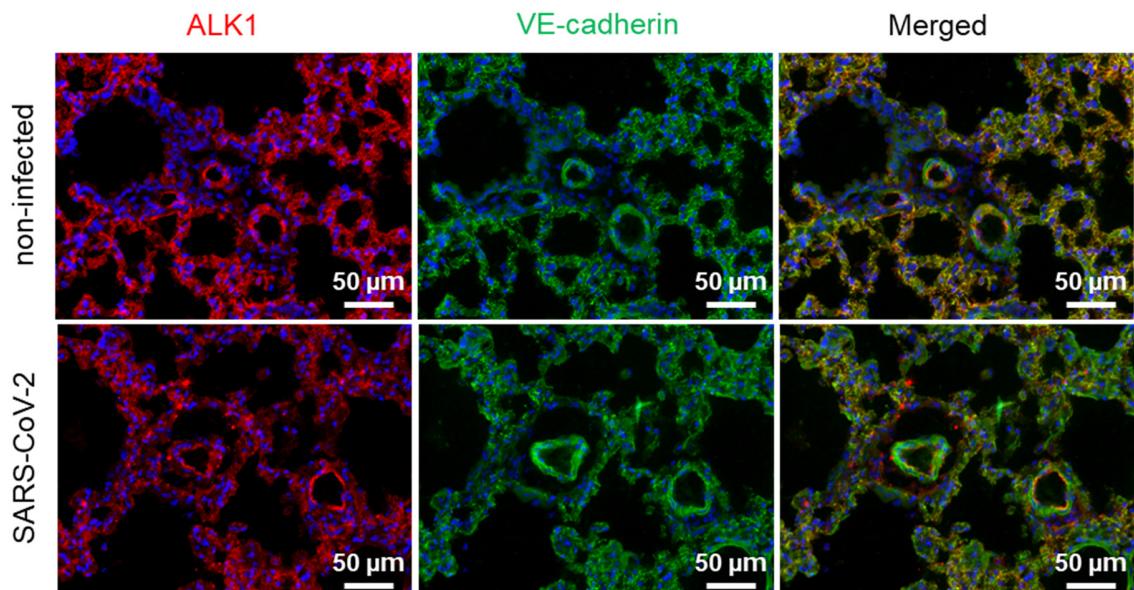
Figure S3. Expression of ALK1 in mouse lung endothelial cells. Immunofluorescent staining for ALK1 and VE-cadherin using mouse lungs infected with or without SARS-CoV-2.
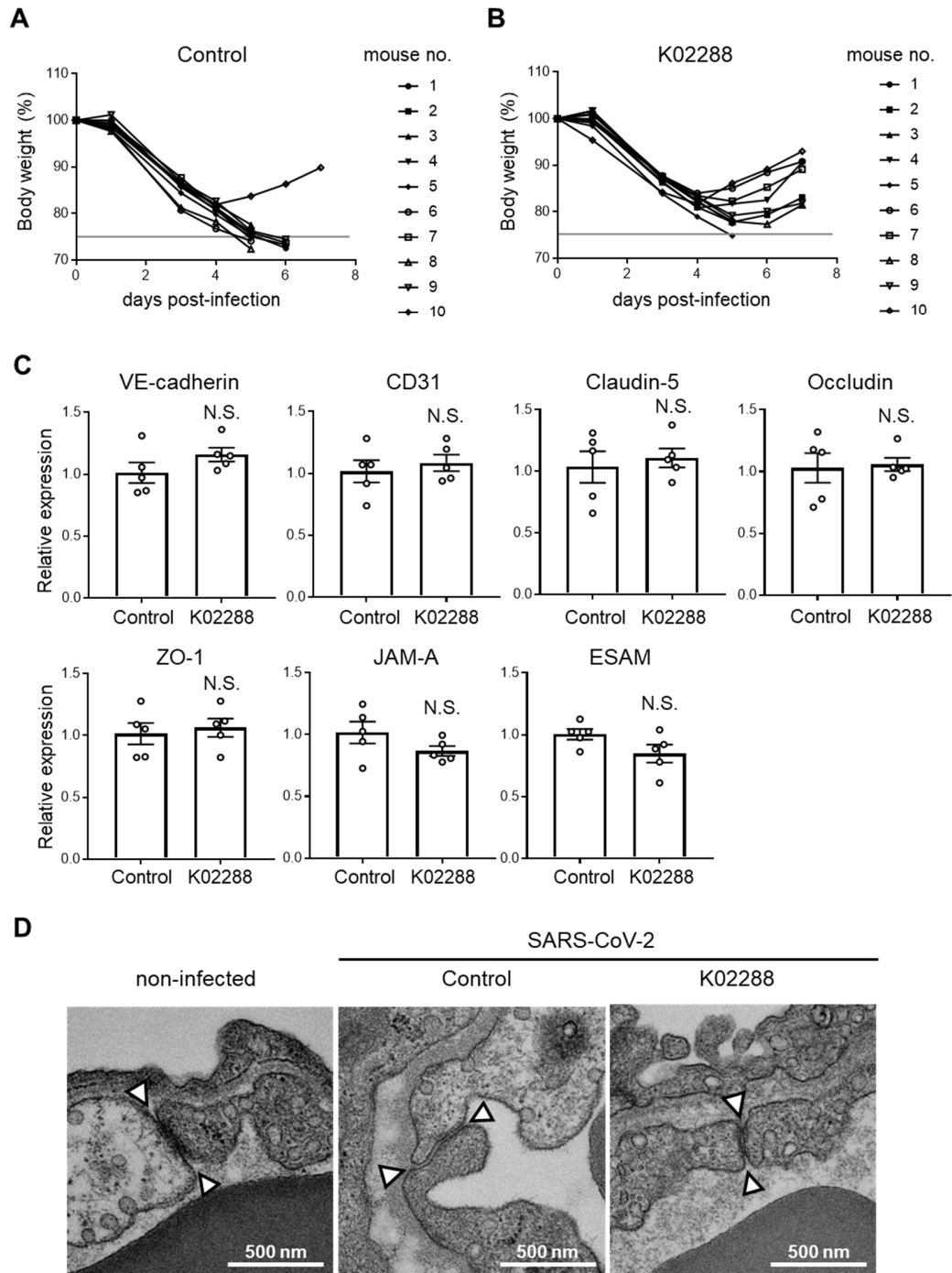
Figure S4. K02288 suppressed body weight loss in SARS-CoV-2-infected mice.

(A, B) BALB/c mice were intranasally inoculated with SARS-CoV-2, and intraperitoneally

injected with vehicle or K02288 (2 mg/kg body weight) in PBS containing 1% DMSO. Body weights of control mice (n = 10) (A) and K02288-injected mice (n = 10) (B) were measured. The humane endpoint was set at 25% body weight loss relative to initial body weight at the time of infection. (C) Expression levels of junction-related genes in SARS-CoV-2 infected mouse lungs with or without K02288 treatment. Four days after the SARS-CoV-2 infection, lungs were harvested from mice with or without K02288 treatment and used for RNA preparation. Expression levels of junction-related genes were measured by qPCR (n = 5, N.S., not significant by the unpaired t-test). (D) Transmission electron microscope (TEM) images of endothelial junctions between in mouse lungs treated with or without SARS-CoV-2 and K02288. Arrowheads indicate the junctions between endothelial cells.

Table S1. Primers used in this study.

Generation of screening cells		5'-3'
Infusion primers	Fw	GTACTTGGAGCGGCCCCTTTCGTCTTCACTCGAG
	Rv	TATTTTATTGCGGCCCACTGATAGGGAGTGGTAA

qPCR primers		5'-3'
human Robo4	Fw	TTATGGCTCCCTCATCGCTG
	Rv	GAGGCTGTCTGAGCTGGAAC
human PAI-1	Fw	GAAGATCGAGGTGAACGAGAGTG
	Rv	ACCACAAAGAGGAAGGGTCTGT
human ID-1	Fw	CTCCAACTGAAGGTCCCTGATGTAG
	Rv	CGACATGAACGGCTGTTACTCAC
human GAPDH	Fw	TGCACCACCAACTGCTTAGC
	Rv	GGCATGGACTGTGGTCATGAG
mouse Robo4	Fw	CTAACAGCTCCCCACTGCTC
	Rv	CTGGGCTTTGAGAAAGGTTC
mouse ALK1	Fw	CTCAGTCACAATCCAGAGAAGCC
	Rv	ACACTCTCTTCACTCCCTCTAC
mouse GAPDH	Fw	TGCACCACCAACTGCTTAG
	Rv	GGCATGGACTGTGGTCATGA
SARS-CoV-2	Fw	AGCCTCTTCTCGTTCCTCATCAC
	Rv	CCGCCATTGCCAGCCATTC
mouse VE-cadherin	Fw	TACTCAGCCCTGCTCTGGTT
	Rv	GCTTGCAGAGGCTGTGTCTT
mouse CD31	Fw	ACGAGCCCAATCACGTTTCAG
	Rv	AAAACGCTTGGGTGTCATTCA
mouse Claudin-5	Fw	CTGGACCACAACATCGTGAC
	Rv	AGTGCTACCCGTGCCTTAAC
mouse Occludin	Fw	TTGAAAGTCCACCTCCTTACAGA
	Rv	CCGGATAAAAAGAGTACGCTGG
mouse ZO-1	Fw	GCCGCTAAGAGCACAGCAA

	Rv	TCCCCACTCTGAAAATGAGGA
mouse JAM-A	Fw	TCTCTTCACGTCTATGATCCTGG
	Rv	TTTGATGGACTCGTTCTCGGG
mouse ESAM	Fw	TTGCTGCGGGTTTTGTTCCT
	Rv	TCTACCGCTTCCAATTTGTTGAG

Genotyping primers		**5'-3'**
CAG-stop^{flox}-Robo4 mouse	Fw	CCATCAAGCTGATCCGGAAC
	Rv	GTAACAGGAGGGTCCCATCC
CDH5-CreERT2 mouse	Fw	GCCTGCATTACCGGTCGATGCAACGA
	Rv	GTGGCAGATGGCGCGGCAACACCATT